Published in final edited form as:

J Physiol. 2021 December ; 599(23): 5261–5279. doi:10.1113/JP282064.

Vagus nerve stimulation activates nucleus of solitary tract neurons via supramedullary pathways

Coty M. Cooper[1], **Ariana Q. Farrand**[1], **Michael C. Andresen**[2], **Eric Beaumont**[1]

[1]Department of Biomedical Sciences, Quillen College of Medicine, East Tennessee State University, Johnson City, TN, 37614

[2]Oregon Health & Science University, Portland, OR, 97239.

Abstract

Vagus nerve stimulation (VNS) treats patients with drug-resistant epilepsy, depression and heart failure, but the mechanisms responsible are uncertain. The mild stimulus intensities used in chronic VNS suggest activation of myelinated primary visceral afferents projecting to the nucleus of the solitary tract (NTS). Here, we monitored the activity of second and higher order NTS neurons in response to peripheral vagal activation using therapeutic VNS criteria. A bipolar stimulating electrode activated the left cervical vagus nerve, and stereotaxically-placed, single tungsten electrodes recorded unit activity from the left caudomedial NTS of chloralose-anesthetized rats. High-intensity single electrical stimuli established vagal afferent conduction velocity (myelinated A-type or unmyelinated C-type) as well as synaptic order (second vs higher order using paired electrical stimuli) for inputs to single NTS neurons. Then, VNS treatment was applied. A mid-collicular knife cut (KC) divided the brainstem from all supramedullary regions to determine their contribution to NTS activity. Our chief findings indicate that the KC reduced basal spontaneous activity of second order NTS neurons receiving myelinated vagal input by 85%. In these neurons, acute VNS increased activity similarly in Control and KC animals. Interestingly, the KC interrupted VNS activation of higher order NTS neurons and second order NTS neurons receiving unmyelinated vagal input, indicating that supramedullary descending projections to NTS are needed to amplify the peripheral neuronal signal from VNS. The present study begins to define the pathways activated during VNS and will help to better identify the central nervous system contributions to the therapeutic benefits of VNS therapy.

To whom correspondence should be addressed: Eric Beaumont, Ph.D., Department of Biomedical Sciences, East Tennessee State University, Johnson City, TN. beaumont@etsu.edu.

Author contributions

Coty Cooper: Acquisition, analysis, and interpretation of data for the work; Drafting the work and revising it critically for important intellectual content; Final approval of the version to be published; Agreement to be accountable for all aspects of the work

Ariana Farrand: Analysis and interpretation of data for the work; Revising the work critically for important intellectual content; Final approval of the version to be published; Agreement to be accountable for all aspects of the work

Michael Andresen: Conception and design of the work; Drafting the work and revising it critically for important intellectual content; Final approval of the version to be published; Agreement to be accountable for all aspects of the work

Eric Beaumont: Conception and design of the work; Acquisition, analysis, and interpretation of data for the work; Drafting the work and revising it critically for important intellectual content; Final approval of the version to be published; Agreement to be accountable for all aspects of the work

All persons designated as authors qualify for authorship, and all those who qualify for authorship are listed.

Author conflicts/competing interests

The authors have no competing interests.

Keywords

nucleus of the solitary tract; vagal primary afferents; vagus nerve stimulation; in-vivo electrophysiology; rats

Introduction

The development of vagus nerve stimulation (VNS) as a device-based therapy has accelerated the demand for a greater understanding of the vagal afferents and how they contribute to central nervous system (CNS) functions. The cervical vagus nerve where stimulation devices are commonly implanted contains predominantly afferent (~80%) axons. Myelinated A-fiber axons are highly sensitive to electrical currents compared to unmyelinated C-fibers, but myelinated afferents account for only 10-15% of total vagal afferents (Andresen et al., 2012). The vagus nerve serves well-established major roles in autonomic and neuro-endocrine-immune regulatory pathways (Cersosimo and Benarroch, 2013). Clinical activation of the vagus nerve provides a surprisingly broad range of potential benefits for patients including epilepsy, depression, cardiovascular disease and immune responses, implicating CNS engagement (Bonaz et al., 2013; Johnson and Wilson, 2018). Pre-clinical and clinical trial work indicate that VNS therapy beneficially treats heart disease (DiCarlo et al., 2013; Premchand et al., 2014; Beaumont et al., 2015; Schwartz et al., 2015; Beaumont et al., 2016; Byku and Mann, 2016; Libbus et al., 2016; Nearing et al., 2016; Premchand et al., 2016; DiCarlo et al., 2018). VNS therapy for epilepsy indicates prevention of seizures in most patients and seizure freedom increases over time, demonstrating the importance of chronic modulation of central pathways (Englot et al., 2016). Despite growing evidence of efficacy and involvement of actions within the CNS, many questions remain regarding the mechanistic basis for VNS benefits.

Based on clinical guidelines for effective stimulus parameters (Premchand et al., 2014; Premchand et al., 2016), we reported that only myelinated vagal afferents were directly activated by VNS (Beaumont et al., 2017). Surprisingly, such VNS also indirectly activated central neurons including second order NTS with non-myelinated vagal afferent contacts as well as polysynaptically-innervated NTS neurons. This “spontaneous” action potential activity was weakly time-linked to VNS (Beaumont et al., 2017). NTS neurons extensively project to many other brainstem and forebrain structures, and many of these regions also project back to NTS, demonstrating potentially important reciprocal pathways (Zhukova, 1980; Loewy, 1990; Karimnamazi et al., 2002; Ulrich-Lai and Herman, 2009; Andresen and Paton, 2011; Affleck et al., 2012; Kawai, 2018; Gasparini et al., 2020). We hypothesized that these anatomical interconnections might be responsible for this amplification of NTS activity via reverberation from supramedullary regions (Cunningham et al., 2008).

The present studies were designed to examine whether CNS pathways are responsible for augmented activity of NTS neurons during low-intensity (clinically-graded) VNS treatment. We assessed NTS events triggered directly by vagal afferents as well as action potentials only loosely linked to vagal stimuli. The timing of events in relation to vagal stimuli allowed us to discriminate direct (i.e. evoked action potential activity) from indirect activation (i.e.

spontaneous action potential activity), and we classified recorded NTS neurons as either second or higher order in relation to vagal afferent fiber type. The augmented activity in NTS neurons associated with therapeutic levels of VNS were nearly eliminated in animals with a mid-collicular knife cut (KC). Briefly, the KC substantially reduced spontaneous activity in all NTS neurons receiving vagal afferent input. Importantly, KC abolished the normal increase in activity induced by VNS in higher order neurons during VNS as well as in second order NTS neurons receiving unmyelinated vagal afferents. Thus, the data implicate neurons of supramedullary origin in the substantial augmentation of NTS activity by VNS and indirectly demonstrate that supramedullary neurons are strongly activated by VNS for sustained periods during VNS therapy.

Materials and Methods

Ethical Approval.

All procedures were approved by the University Committee on Animal Care of East Tennessee State University (ETSU) in Johnson City, Tennessee (protocol: P181101). These animals were kept according to guidelines set in the *Guide for the Care and Use of Laboratory Animals*, Eighth Edition, National Academy Press, Washington DC, 2011. All experiments were designed in order to limit pain and distress of the animals as well as number of animals required. The investigators conducting this study have reviewed *The Journal of Physiology*'s ethical principles and confirmed that this animal work complies with that checklist.

Animals.

Rats were kept in a facility at ETSU accredited by the Association for Assessment and Accreditation of Laboratory Animal Care. This facility is registered with and periodically inspected by the United States Department of Agriculture. Twenty-three male Sprague-Dawley rats (Envigo, IN) weighing approximately 360 g (12-13 weeks old) were housed under a standard 12-hr light/dark cycle with food and water provided *ad libitum*. Rats were randomly divided into 3 groups for this study: 10 Control rats, 10 KC rats, and 3 additional Control rats for hypothalamic paraventricular nucleus (PVN) activation experiments (see below for details).

Surgical preparation.

Anesthesia was induced with 3% isoflurane using an induction chamber (VetEquip Inc., CA) and maintained by a nose cone. Sufficiency of anesthesia was monitored by absence of both hindlimb toe-pinch responses. The jugular vein was cannulated for the administration of α-chloralose anesthetic. Electrocardiogram (ECG) was used to monitor heart function (model P511, Grass Instrument Company, MA). The trachea was cannulated and mechanical ventilation was maintained with a positive pressure of 12 to 14 mm of H_2O using 100% O_2 at a tidal volume of 2-3 ml and 60 breaths per minute (SAR-830/P ventilator, IITC Inc., CA). Expired CO_2 level was maintained at 3% by adjusting the inspiration pressure (CWE, CapStar-100, PA). A feedback-controlled heating blanket (Harvard Apparatus, Canada) maintained rectal temperature at 37°C.

VNS preparation.

Our setup in rats mimicked as much as possible the clinical practice in which cervical VNS in patients targets the vagosympathetic trunk (Seki et al., 2014). Our bipolar cuff electrodes (Nano-Fiber Fusion, FNC-500-V-R-2C-30, Micro-Leads, MA) were positioned similarly, and the cuff was wrapped around the left cervical vagus nerve, the aortic depressor nerve and the sympathetic nerve using a ventral approach. The cuff-externalized lead wires were connected to a stimulus generator through an isolation unit (AMPI Master 9, Israel). Experimental protocols are described below.

Stereotaxic preparations.

Following ventral wound closure, the rat was positioned prone in a stereotaxic frame with ear bars and a mouthpiece to accommodate the dorsal approach to NTS recording. The head of the rat was tilted forward at ~ 30° to facilitate access to the dorsal surface of the medulla oblongata without the need to remove the cerebellum. The NTS region was exposed rostrocaudally from the calamus scriptorius to the rostral aspect of the area postrema. The exposed brain area was covered with mineral oil to prevent drying. When all surgical procedures were completed, anesthesia was switched to maintenance with α-chloralose starting with a slow bolus injection (IV, 50 mg/kg) given over 20 minutes. Following completion of the slow bolus of α-chloralose, isoflurane administration was ceased and a low-volume, continuous infusion of α-chloralose maintained the anesthetic state (IV, 30 mg/kg/hr). Depth of anesthesia was periodically confirmed throughout experiments by absence of both hindlimb toe-pinch responses. Thirty minutes were allowed for the animal's heart rate to stabilize prior to neural recordings or VNS interventions.

KC procedure.

In a subset of rats, we used a KC to separate the brainstem from supramedullary portions of the brain (n=10 KC rats). The top surface of the rat's skull was positioned horizontally, and a midline incision was made with a scalpel, beginning rostral to the coronal sutures of the skull and extending to the second cervical vertebrae. The periosteum covering the skull was retracted, and a cotton swab was used to remove any blood on the surface of the skull. Bregma was identified, a measurement of 9.0 mm caudally was marked at the midline, and a Micro Drill (Foredom, CA) equipped with a burr bit (FST, CA) was used to create a slit across the cranium. A triangular surgical microblade was then inserted in the slit and moved bilaterally to transect the brain. We previously demonstrated that this procedure preserves NTS function in rats including baroreflex function (Lee et al., 2002).

PVN activation.

In a separate group of Control rats (n=3), the top surface of the skull was positioned horizontally, and a midline incision was made with a scalpel. Bregma was identified, and a Micro Drill was used to create a hole in the skull over the PVN area using the following coordinates: 1.8 mm caudal, 0.5 mm lateral and a depth of 7.5 mm in relation to Bregma. Then, a concentric bipolar electrode was positioned in the ipsilateral left PVN for activation with 100 μA electrical stimuli at 1 Hz for 20 s.

NTS recording.

Extracellular neural activity was recorded using high impedance (1 MΩ) tungsten electrodes (FHC, ME) positioned stereotaxically and driven by a 3D micromanipulator (Patchstar, Scientifica, UK). The tungsten electrode was lowered slowly into the caudal portion of the left medial NTS, at the caudal tip of the area postrema, 0.2-1.5 mm laterally from midline and 0.5-1.3 mm ventral to the dorsal surface following published coordinates (Paxinos et al., 1985; Paxinos and Watson, 1986). In a differential recording against remote ground and reference electrodes placed in posterior neck muscles, the neural signal was amplified, passed through a filter (bandwidth setting 0.1-3 kHz; A-M Systems Model 1800, WA), and processed to remove 50-60 Hz noise along with its harmonics using a Hum-Bug filter (Quest Scientific, Canada). Filtered signals were sampled using a CED acquisition system with Spike 2 software version 9.04 (CED, England) at the rate of 20 kHz for neural signals and 1 kHz for ECG.

Experimental protocols.

1) Neuronal Search Test.—Vagal stimulus parameters were based on pilot studies indicating that a high-intensity stimulus (~ 3.5 mA) activated all myelinated and unmyelinated vagal afferent axons and is thus supramaximal (not shown). Fine adjustments of electrode tip depth improved the evoked spike signal (signal/noise ratio > 3/1). Following optimization, the electrode position was held fixed for the remaining protocols. The conduction velocity of vagal afferents was estimated from the arrival time (latency) divided into the conduction distance, resulting in unmyelinated C-fiber conduction velocities of < 2 m/s, whereas effective conduction velocities > 3.5 m/s were consistent with myelinated A-fiber conduction. Neurons encountered that did not respond with evoked action potentials to high-intensity stimuli were not further studied.

2) NTS unit identification.—To assess the characteristic latency and jitter (SD of latency) of identified vagus-responsive NTS neurons, 20 vagal electrical stimuli were delivered at 0.3 Hz using a pulse width of 100 μs. Each vagal pulse iteration triggered a single sweep-within-oscilloscope mode in Spike 2, setting the 0 time point at the electrical stimulus to determine the latency to the detected evoked action potentials (eAP). We defined a Bracket of Arrival for each neuron as the range of latencies, measured from the onset of the vagus stimulus artifact to the half-height of the unit eAP. After each experiment, unit eAPs were scanned with Spike 2 software to create a principal component analysis (PCA) template. Following determination of the characteristic PCA template for each NTS unit, the entire record for that neuron was analyzed to identify spontaneous activity (sAP) corresponding to the PCA template during baseline and stimulation periods. Finally, the record was manually inspected across the full recording to reject any counts of rare artifacts falling within the PCA limits. Practically, specific templates reliably identified consistent waveforms attributed to individual NTS neurons (Beaumont et al., 2013; Beaumont et al., 2017). The analyses were limited pragmatically to simultaneous recognition of up to three unique NTS neurons per recording site.

3) Mono vs polysynaptic pathways from the vagus.—To determine the likely synaptic pathway between the recorded NTS neuron and its vagal afferent input, high-

intensity supramaximal stimuli were delivered as a pair of electrical stimuli (5 ms interstimulus interval, 200 Hz). Neurons in which each of the paired electrical stimuli successfully triggered an eAP were considered directly connected to the vagus (i.e. monosynaptic). Alternatively, NTS neurons receiving a polysynaptic input failed to elicit an eAP coinciding with the second electrical stimulus of the paired pulse (Andresen and Kunze, 1994; Scheuer et al., 1996).

4) VNS treatment.—A major treatment in our studies was to activate the vagus nerve with a stimulus styled to replicate the clinical settings used in VNS therapy. A bradycardic intensity (BI) was established for each rat by determining the minimal current during 20 Hz VNS that elicits a 5% bradycardia. Note that the determination of BI accounts for variations in each nerve trunk and electrode conditions across preparations. The BI intensity for control rats was 0.24 ± 0.21 mA (range 0.11 – 0.75) and was found to be similar to KC rats' BI intensity, which was 0.21 ± 0.25 mA (range 0.22 – 0.68)) (*t* test, P = 0.4552). During VNS treatment periods, BI-level stimulation was initiated, delivering five successive cycles (VNS/off period), consisting of a 14 s VNS period at 20 Hz followed by an off period of 44 s. The pulse duration was set at 100 μs. Following completion of these protocols, the Search Test was reinitiated and the microelectrode advanced to find additional vagally-activated NTS neurons. Following data collection, rats were euthanized by adding 5% isoflurane during mechanical ventilation until pinch reflexes were eliminated, followed by exsanguination.

Statistical analysis.

Individuals analyzing NTS data files were blinded to the rats' treatment groups (i.e. Control or KC). For each NTS neuron, the baseline activity was calculated by averaging sAP for 60 s preceding the 5 VNS cycles. For each VNS cycle, we counted APs (distinguishing eAPs from sAPs) and divided this number by the period of time for each active VNS period (14 s) and each off period (44 s) to generate an average neuronal activity value (in Hz). Note that only neurons that increased their activity level by ≥30% above baseline during VNS were considered responsive to VNS (Responder neurons). The Shapiro-Wilk test assessed the normality of the data distribution before applying within-group and between-group comparisons. All the data comparisons included in the study exhibited a normal distribution. The assumption of sphericity was verified by Mauchly's test, and the Greenhouse-Geisser correction was applied when this assumption was violated.

The average rates of eAP or sAP for baseline and five consecutive cycles (VNS/off period) of VNS were compared within each animal group for each type of NTS neuron (receiving input from monosynaptic A-fiber vagal afferents, i.e. A-fiber Mono, monosynaptic C-fiber vagal afferents, i.e. C-fiber Mono, or polysynaptic vagal afferents, i.e. Poly). These comparisons were examined using a repeated-measures analysis of variance (RM ANOVA), and Dunnett's post hoc tests were used to compare pairs of means for each VNS cycle with the baseline. Effect sizes were calculated as partial eta squared (η_p^2) from the ANOVA. Independent *t* tests were used to compare: 1) the latency distribution for each neuronal type (A-fiber Mono, C-fiber Mono and Poly), 2) baseline activity level between Control and KC rats, 3) BI between Control and KC rats, 4) heart rate before and after the KC and 5) base

vs 40 s for PVN stimulation. All statistical analyses were performed using SPSS, version 25.0 (IBM Corp., NY). For all statistical comparisons, $P < 0.05$ was considered statistically significant. In the text and in the figures, results are reported as the mean ± SD.

Results

Identification of vagally-activated NTS neurons.

In vagus-responsive NTS neurons, high-intensity electrical stimuli to the cervical trunk of the vagus elicited eAPs directly related to each electrical stimulus during the Search Test. These successful eAPs were used to construct a PCA template that identified all APs originating from a single NTS neuron. The arrival times of the vagally-activated NTS eAPs (latency) were consistent for each neuron, even with closely timed (5 ms) pairs of vagal electrical stimuli (Figure 1). All spikes satisfying the PCA template but arriving outside of the Bracket of Arrival were considered sAP of that unique neuron (gray circle, Figure 1). Monosynaptic eAPs followed pairs of electrical stimuli similarly (filled circles, Figure 1) with narrow PCAs, regardless of conduction class (Figure 1). In contrast, polysynaptic vagal connections arrived later with no second eAP corresponding to the second paired electrical stimulus, indicating activation failure (unfilled circles, Figure 1). Thus, two classes of vagal responses were defined by the paired pulse tests – monosynaptic and polysynaptic.

The AP arrival time reflects the nature of the vagal afferent pathway (Beaumont et al., 2017), and the vagal afferent pathway performance within NTS was a major goal of our studies. The high-intensity supramaximal electrical stimuli to the vagus activated a single AP for each stimulus falling within the PCA composite bounds over 20 iterations at 0.3 Hz. In Control rats (n=10), these Search Tests activated a total of 83 NTS neurons. The arrival time variation was expressed as the SD of the latency (or eAP jitter). The earliest arrival times corresponded to vagal A-fiber afferents in Control rats and were grouped tightly in single, normal distributions for each neuron with latencies averaging 6.5 ± 1.2 ms. Vagal afferent A-fiber pathways had characteristically minimal jitter (mean = 1.2 ± 0.63 ms, individual jitters indicated in Figure 2 as horizontal SD bars). These performance features are consistent with monosynaptic myelinated A-fiber vagal afferent inputs (A-fiber Mono, Figure 2, grey, n=8). A second group of low-jitter, monosynaptic vagal inputs were similarly grouped within single, normal distributions for each neuron, but the latencies for these neurons were more broadly distributed across a wide range of arrival times and corresponded to monosynaptic vagal C fiber afferents (C-fiber Monos). C-fiber Monos were far more common than A-fiber pathways (C-fiber Mono, Figure 2, red, n=46). The latency for C-fiber-receiving NTS neurons for the Control group averaged 22.8 ± 3.4 ms (jitter of 3.4 ± 1.64 ms). Thus, about 10% of the monosynaptic vagal neurons were connected to A-fibers (8/83), which is consistent with our previous work (Beaumont et al., 2017). The latest-arriving set of vagal inputs had eAPs with very large jitters and succeeded in activating an action potential to the first (but not the second) electrical stimulus of the paired pulse test. These failures to the paired pulse test identified these neurons as receiving vagal afferent inputs following a polysynaptic pathway within NTS (Poly, blue, Figure 2, n=29). NTS Poly neurons were less commonly encountered than C-fiber Monos, and in the Control group averaged 34.8 ± 14.3 ms (jitter of 14.3 ± 2.96 ms). The distribution of each of these response

groups was well-fit by a normal distribution of latencies for each category (Figure 2, top panel). The jitter was significantly different between A-fiber Monos, C-fiber Monos and Polys using an ANOVA (P = 0.0011). Note that no NTS neuron responded with multiple stimulus-synced eAPs using these protocols despite supramaximal intensities. Together, these tests identified three vagus-responsive classes of NTS neurons (A-fiber Monos, C-fiber Monos and Polys) that responded to high-intensity stimuli with distinct arrival times, latency jitters and failure/fidelity characteristics indicative of vagal afferent processing within NTS.

VNS treatment increased NTS neuron activity.

The high-intensity Search Test stimuli established the unique performance characteristics of multiple classes of vagus-responsive NTS neurons. VNS treatment was intermittent as in therapeutic application and triggered both eAPs and sAPs in vagally-innervated NTS neurons (Figure 3). Note that the stimuli delivered at BI during VNS treatment were much weaker than the intensity of Search Test stimuli. These weak electrical stimuli delivered at BI (Figure 3, bottom) directly activated eAPs only in A-fiber Mono neurons (Figure 2). On close examination, eAPs occurring during VNS fell within a narrow Bracket of Arrival (filled circles, Figure 3 bottom). Failures to evoke eAPs within the expected Bracket of Arrival were evident as well (Figure 3, bottom). Though these failures occurred frequently, other APs corresponding to the same neuron were consistently detected outside the limits of the Bracket of Arrival and were deemed sAP (Beaumont et al., 2017) (Figure 3 bottom). Note that often multiple, unique action potential profiles, each with their own PCA template, could be discriminated at a single electrode site, allowing identification and assessment of up to three separate NTS neurons simultaneously.

VNS treatment directly activated A-fiber second order NTS neurons.

VNS treatment directly activated eAPs in all 8 A-fiber Mono NTS neurons identified in Control rats. Thus, the BI determined in each animal was suprathreshold for vagal A-fiber activation. Note, however, that the success rate of eAPs (number of triggered eAPs / number of VNS stimuli delivered) for BI VNS ranged from 35-40% across all five VNS periods at 20 Hz (Figure 4, left). VNS treatment itself did not affect the stimulus threshold since the eAP success rate was unchanged over the five cycles (ANOVA, P = 0.1525, $\eta_p^2 = 0.227$). Thus, BI electrical stimuli delivered in this way failed to evoke APs ~65% of the time. This can be considered the actual throughput between the myelinated vagal afferent axons. Note that only eAPs will be conducted beyond these A-fiber Mono NTS neurons. VNS treatment did not increase sAP over successive cycles or above Baseline activity in A-fiber Mono NTS neurons (ANOVA, P = 0.2978, $\eta_p^2 = 0.148$, n=8, Figure 4, right). The BI level of VNS was subthreshold for C-fiber vagal afferents and failed to directly activate eAPs in NTS C-fiber Mono neurons (see below for full analysis of these neurons). Thus, all VNS-induced activity changes, including indirect responses in NTS neurons, were initiated solely by vagal A-fiber activation of their second order neuron sources.

KC decreases activity in NTS and reduces VNS direct activation.

The mid-collicular KC (9.0 mm caudal from Bregma) eliminated all ascending and descending connections between the brainstem and the forebrain (Figure 5, top schematic). BI was determined from the heart rate responses for each rat before proceeding to KC

surgery. Immediately following the KC procedure, each animal's heart rate was variable for ~ 5 minutes, but stabilized within 30 minutes after the KC before redetermining BI or beginning recordings of NTS neurons. Heart rates were similar pre- (329 ± 17 bpm) and post-KC (341 ± 22 bpm) procedure (*t* test, P = 0.3812, n=10). BI was identical before and after the KC procedure for all animals (n=10). Since the KC surgery requires manipulation of the brain, Control and KC recordings were performed in different animals (n=10 KC rats – 62 NTS neurons). The KC dramatically reduced the overall activity in NTS neurons (Figure 5, bottom graphs).

In searching for NTS neurons coupled to vagal afferents, we used the same criteria in KC rats as in intact Control animals. The NTS neurons in KC rats were classified into 3 classes based on their vagal afferent coupling (A-fiber Mono, C-fiber Mono and Poly, Figure 6) and showed quantitatively similar prevalence to that of Control rats. The distributions for each of the NTS cell classes overlap (Figure 6 compared to Figure 2), with similar normal distributions within each class. NTS neuronal classes divided along the same latency and jitter values characteristically (A vs C), but neither the mean latency nor mean jitter values were different in KC compared to Controls. Indeed, A-fiber Mono characteristics were similar: Control latencies: 6.5 ± 1.2 ms (jitter 1.2 ± 0.63 ms, n=8) vs. KC: 7.4 ± 0.95 ms (jitter 0.95 ± 0.31 ms, n=4) (*t* test, P = 0.4015). Likewise, C-fiber Mono neurons were similar between groups: Control latencies: 22.8 ± 3.4 ms (jitter 3.4 ± 1.64 ms, n=46) vs. KC: 22.2 ± 3.5 ms (jitter of 3.5 ± 1.37 ms, n=35) (*t* test, P = 0.7051). Polysynaptic in Controls (34.8 ± 14.3, jitter 14.3 ± 2.96 ms, n=29) were also similar to KC (41.0 ± 15.3 ms, jitter 15.3 ± 4.71 ms, n=23) (*t* test, P = 0.1525). The absence of significant difference in each afferent pathway class (compare Figure 2 to Figure 6) indicates that the basic performance characteristics of the mono- and polysynaptic vagal afferent conduction paths to NTS neurons were unaffected by the KC.

The basic vagal afferent pathway connections within the brainstem remained intact after KC. Thus, vagal stimuli at BI successfully triggered eAPs in A-fiber Mono NTS neurons during the periods of active VNS stimulation in both Control and KC animals (Figure 7). However, the mean success rates for A-fiber Mono inputs in response to the 20Hz VNS stimuli fell significantly from ~ 7 Hz (success rate of 35%) in Controls to ~ 3 Hz (success rate of 15%) in KC rats (ANOVA, P < 0.0001, η_p^2 = 0.333, n=12 neurons). Thus, the vagal connections remained intact, but their translation into APs was much lower without feedback from supramedullary neurons following KC. Successive VNS bursts of stimuli from VNS 1 to VNS 5 had no effect on success rate of transmission in either Control (Control: ANOVA, P = 0.2978, η_p^2 = 0.148, n=8 neurons) or KC rats (KC: ANOVA, P = 0.1605, η_p^2 = 0.399, n=4 neurons).

In addition to eAP activity during the active stimulation periods of VNS, substantial sAP activity occurred during active stimulation periods. The rate of sAP activity in A-fiber Mono varied little across active VNS periods 1-5 for Control rats (ANOVA, P = 0.0704, η_p^2 = 0.347, n=8) and KC rats (ANOVA, P = 0.3626, η_p^2 = 0.147, n=4, Figure 8, top). The sAP was not different between KC and Controls during VNS periods 1-5 (Figure 8 top). Activity levels were similar across Base/off periods in Control (ANOVA, P = 0.5528, η_p^2 = 0.079, n=8) and in KC rats (ANOVA, P = 0.7989, η_p^2 = 0.133, n=4, Figure 8 bottom).

Alternatively, sAP was substantially reduced in NTS neurons from KC rats compared to Control rats for these time periods. The KC operation nearly eliminated the high levels of sAP activity during Base and Off periods 1-5 compared to Controls (ANOVA, $P < 0.0001$, $\eta_p^2 = 0.624$, n=12 neurons). This finding indicates that intact supramedullary connections normally provide a strong tonic excitatory influence on A-fiber Mono NTS neurons during periods of vagal afferent quiescence (base and off periods).

VNS treatment increased indirect activity of C-fiber second order NTS neurons.

High-intensity electrical stimuli activated C-fiber vagal afferents directly connected to a substantial majority of second order NTS neurons (46 of 54 second order neurons). However, mild, BI-level electrical stimuli failed to activate eAPs in any of these neurons, i.e. BI electrical stimuli were subthreshold for all C-fiber Mono neurons. Despite this direct evidence that BI activated only myelinated vagal afferents, bursts of sAP activity accompanied each VNS period delivered at BI in ~15% of these vagal C-fiber Mono NTS neurons for Control rats (Figure 9 left), designated as Responder neurons. To qualify as a Responder neuron, sAP was augmented >30% during VNS cycles compared to Base. This detailed analysis utilized the Bracket of Arrival for each monosynaptic input and indicated that this VNS-augmented activity consisted entirely of unsynced sAPs. Responder C-fiber Mono neurons were a minority (15%), and because of the high sAP variability and the low number of neurons, increased sAP averages during active stimulation were not significantly higher compared to the average Base (ANOVA, $P = 0.5680$, $\eta_p^2 = 0.115$, Figure 9 bottom-left). The remainder of C-fiber Mono neurons were Non Responders, and their sAP activity level was unaffected by VNS and remained equivalent to Base (ANOVA, $P = 0.6682$, $\eta_p^2 = 0.085$, Figure 9 bottom-middle). Interestingly, in KC rats only Non Responder vagal C-fiber Mono NTS neurons were observed (ANOVA, $P = 0.7615$, $\eta_p^2 = 0.026$, n=35, Figure 9 bottom-right).

VNS treatment increased indirect activity of polysynaptic neurons.

Poly neurons encountered in NTS were only indirectly coupled to vagal afferents. Poly-coupled NTS neurons showed distinct increases in sAP activity in response to high-intensity vagal electrical stimuli (Figure 2), with no evidence of direct synaptic coupling to vagal afferents either at high-stimulus intensities or at BI (Figure 10). In such higher order NTS neurons in Control rats, ~60% (17/29) of these neurons were Responders to VNS treatment at BI with increases in sAP activity > 30% during VNS periods compared to Base (ANOVA, $P = 0.0138$, $\eta_p^2 = 0.208$, Figure 10 bottom-left) and also off periods compared to Base (ANOVA, $P = 0.0053$, $\eta_p^2 = 0.569$, Figure 10 bottom-left). No Responder class of Poly NTS neurons were found in KC rats (n=23, Figure 10, bottom right). The sAP activity of Non Responder neurons did not change during VNS either in Control (n=12, ANOVA, $P = 0.3212$, $\eta_p^2 = 0.147$, bottom-middle) nor in the entire subset of Non Responders in KC rats (n=23, ANOVA, $P = 0.1236$, $\eta_p^2 = 0.220$, bottom-right). This overall result suggests that most (~60%) higher-order NTS neurons are activated by VNS treatment in Controls. Higher order neurons responded to VNS more frequently (~60%) compared to the C-fiber Mono NTS neurons (~15%). As with C-fiber Mono NTS neurons, supramedullary connections are responsible for VNS activation of Poly NTS neurons (Figure 10, bottom-right) since all recorded Poly NTS neurons for KC rats are Non Responders.

Activation of PVN triggered increased NTS activity.

The KC surgery is a crude severing of connections separating brainstem from forebrain nuclei and pathways. Among the suspected contributing nuclei is the PVN. PVN 100 μA electrical stimuli (at 1 Hz for 20 s) activated 7/12 NTS neurons. NTS activity did not increase immediately with PVN activation. Instead, in all cases, NTS activity increased slowly during PVN stimulation and stayed elevated for up to 20 s after stimulation ceased (two sample t test, Base vs 40 s, P = 0.0353, Figure 11). These 7 activated neurons were polysynaptically coupled to vagal inputs, while the 5 PVN-unresponsive neurons were monosynaptically coupled to unmyelinated vagal inputs (C-fiber Monos). None of the observed APs satisfied our criteria for direct synchronization to PVN electrical stimuli. Thus, PVN neuronal activation leads to increased sAP for a substantial portion of Poly NTS neurons.

Discussion

Vagus nerve stimulation has entered the clinic and yet its fundamental basis is poorly understood. The present study was designed to evaluate whether supramedullary neurons contributed to neuronal activity in NTS during VNS treatment. Thus, we hypothesized that supramedullary neurons were activated by vagal A-fiber afferent activity during VNS treatment, and the descending connections from these supramedullary neurons spread excitation to other NTS neurons. Our studies divided the recorded NTS neurons into three classes based on vagal afferent coupling: A-fiber Mono, C-fiber Mono and Poly. Our chief findings show that therapeutic intensities of VNS: 1. Directly evoked APs only in NTS neurons monosynaptically contacted by vagal A-fiber sensory axons. 2. Indirectly activated a proportion of C-fiber Mono and Poly neurons within NTS. 3. Activated supramedullary neurons and their connections back to neurons within NTS. Our studies in KC rats indicate that supramedullary neurons are required for the indirect activation of sAPs in C-fiber Mono and Poly NTS neurons. Not only do these sAP responses to VNS involve descending inputs from supramedullary neurons connected to NTS, but the KC eliminated pathways that reduced the success rate of vagal afferent transmission. Thus, these supramedullary pathways have a tonic influence on basic vagal viscerosensory transmission in NTS. Our attention to the variation in AP latencies and the use of graded intensity of vagal stimulation were key experimental design aspects fostering our conclusions. These brainstem-supramedullary connections are also responsible for spreading discrete myelinated vagal afferent excitation to a subset of intrinsically C-fiber vagal afferent-defined pathways, thereby amplifying the VNS-induced augmentation of NTS activity. These new results offer new perspectives on vagal afferent signaling and evidence of amplification of the VNS-initiated A-fiber signal.

VNS activates pathways beyond the brainstem.

Our studies were designed to test the influence of supramedullary neurons and their connections on activity within NTS. Our key maneuver was relatively crude but simply severed the connections between the forebrain and the brainstem so that we could monitor changes in vagal afferent activation of NTS neurons. Our previous work surprisingly suggested that selective activation of A-fiber vagal afferents indirectly activated APs in

NTS neurons that could not be directly attributed to those afferent connections within NTS (Beaumont et al., 2017) . These increased APs during VNS therapy were poorly synced to the time of each vagal stimulus and thus considered indirectly activated. As with this previous work, we used high-intensity stimuli to the cervical vagus to identify three classes of vagus-responsive NTS neurons – monosynaptically-connected second order NTS neurons with A-fiber or C-fiber input and a third group that were polysynaptically connected to the vagus. Thus, we studied different aspects of NTS vagal processing that represent different pathways from vagal afferent to each NTS neuron. All responses suggested that single vagal inputs drive the activation and timing of evoked action potentials consistent with either A-fiber or C-fiber monosynaptic vagal afferent connections. In second order neurons, no time-dispersed or multiple eAP cases were encountered, indicating that any convergent afferent inputs were unable to doubly excite these second order NTS neurons. This absence of A- and C-fiber convergence was consistent with both in vivo (Beaumont et al., 2017) and in vitro slice (McDougall and Andresen, 2013; Fawley et al., 2021) intracellular recordings of NTS neurons. In second order NTS neurons, additional mechanisms that might prevent rapid re-excitation include a prolonged inhibition of spike generation by the common presence of feedback inhibitory synapses (Miles, 1986; Doyle and Andresen, 2001) or the presence of a strong A-type potassium current (Bailey et al., 2007). Our clinically-defined BI did not directly trigger monosynaptic APs in NTS neurons innervated by C-fibers. Thus, VNS-recruited activity at BI is entirely derived from activation of A-fiber Mono NTS neurons (roughly a 10-20% subset of the NTS population). The VNS-associated increase in AP activity for C-fiber Monos and Poly NTS neurons was entirely indirect and was interpreted in our analysis as sAP. Such findings raise questions about interpreting VNS using highly time-averaged NTS response indicators such as cFOS and calcium imaging since such measures cannot discern direct from indirect activation of vagal afferent pathways accurately.

Mid-collicular transection reduces indirect activation of NTS neurons.

The largest increases of activity in NTS neurons were labeled as sAP in our analysis. These effects were prominent in a subset of NTS neurons monosynaptically activated by vagal C-fibers and in the majority of NTS neurons polysynaptically linked to the vagus. In KCs, this indirect activation of Mono C and Poly NTS neurons was not observed during VNS. Since KCs severed supramedullary pathways to and from NTS, this distinct difference suggests that such pathways are an essential requirement of the indirect VNS-induced increase in NTS activity for these neuronal classes. Such KCs also decreased the fidelity of directly evoked vagal myelinated afferent transmission to NTS. Together the KC changes indicate that the ongoing resting state of NTS neurons is supported by actions of supramedullary neuron activity. Eliminating descending supramedullary inputs by the KC suppressed vagal afferent transmission to NTS second order neurons, and this action may account for a major fraction of the decreased efficacy of VNS to augment sAP activity. In the absence of supramedullary activity, amplification from A-fiber pathways to C-fiber and polysynaptic pathways was not present (Figure 9-10, lower panels). Thus, supramedullary-descending connections expand the overall magnitude of the VNS responses within NTS.

The identity of the supramedullary influences susceptible to KC remains uncertain. Based on many previous anatomical and functional studies, candidate supramedullary brain regions certainly include the PVN. Our direct activation of PVN slowly increased AP activity in a portion of NTS neurons, and the excitation persisted well beyond the period of stimulation in the majority of polysynaptic NTS neurons. Hypoxia inhibits or activates PVN terminals in the NTS and blunts or facilitates cardiovascular responses, respectively (Ruyle et al., 2018). Moreover, activation of PVN often decreases blood pressure, particularly at higher stimulus frequencies (50 Hz) (Yamashita et al., 1987). In our studies, we used a very low stimulus frequency (1 Hz) that did not change heart rate during PVN activation (all rats), suggesting that our observed increases in NTS activity were unlikely to be attributed to a decrease in blood pressure. This indicates that supramedullary neurons normally enhance NTS activity during VNS and enhance the vagal signal to the CNS. Since PVN has reciprocal innervation with NTS neurons, PVN remains a strong candidate for reciprocal excitation of NTS that warrants future evaluation.

Descending connections to NTS from supramedullary neurons are extensive (Loewy, 1990). A major supramedullary region sending GABAergic inputs to NTS is the central amygdala, with additional GABAergic fibers originating from the periaqueductal grey, bed nucleus of the stria terminalis, insula, and parabrachial nucleus (van der Kooy et al., 1984; Loewy, 1990; Kawai, 2018). The impact of GABAergic transmission would be expected to be inhibitory and thus inconsistent with the excitatory effects eliminated by the KC surgery. Additional modulatory neurotransmitters associated with some of these supramedullary neurons including peptides such as oxytocin and vasopressin would also be eliminated by the KC. Although PVN is a prominent supramedullary glutamatergic projection to NTS, additional glutamatergic projections include the lateral hypothalamus and the infralimbic cortex (Kawabe et al., 2008; Geerling et al., 2010; Gasparini et al., 2020). Additional studies are required to determine how each of these projections affects the excitability of NTS neurons.

Vagal afferents enter the CNS directly and predominantly synapse on second order NTS neurons (Andresen and Kunze, 1994). From NTS, vagal information flows broadly across the CNS such that anatomical tracers placed in caudal NTS travel to many central structures, and such connections are often reciprocal, suggesting potential bidirectional communication (Loewy, 1990). The density of these CNS contacts is unequal and dominated by projections to the PVN, the central nucleus of the amygdala, and parasubthalamic nucleus (Gasparini et al., 2020). Some second order NTS neurons project directly out of NTS to other brainstem regions such as the caudal ventrolateral medulla, whereas other brain regions are connected via a mix of vagal second and higher order NTS neurons (Bailey et al., 2006). Thus, NTS neurons can be defined by their position along the pathway of viscerosensory afferent information into the CNS. Our studies have evaluated NTS neurons by functional pathway connectivity in vivo. We followed neuronal responses in temporal relation to vagal afferent activation (latency, jitter and computed conduction velocity). Having an intact nervous system is a critical aspect of our studies, but being limited to extracellular AP timing, we had no direct access to the underlying cellular mechanisms responsible. Intracellular assessments of synaptic transmission indicate that vagal afferent neurotransmitter release is subject to frequency-dependent depletion, GABAergic and peptidergic modulation of release

and terminal depolarization block – all presynaptic processes altering postsynaptic event amplitude (Andresen and Paton, 2011). In addition, postsynaptic membrane changes such as afterhyperpolarization and GABAa receptor activation also affect spike generation – the only extracellular signal reliably detected.

The anatomy, electrophysiology and functional/physiological measures have long supported a major influence of PVN on NTS neurons and vagal afferent pathways including the integration of stress and endocrine signaling (Ulrich-Lai and Herman, 2009; Gonzalez et al., 2021). Early evidence included the presence of unique hypothalamic neuropeptides such as vasopressin and oxytocin within NTS (Sofroniew et al., 1981), participation in neurotransmitter networks (Sawchenko and Swanson, 1983) and a largely excitatory monosynaptic effect of PVN on a large portion of NTS neurons (Kannan and Yamashita, 1985). For example, oxytocin and vasopressin are released within the NTS region by PVN activation (Landgraf et al., 1990). Within the context of this extensive body of work, our tests with electrical activation of PVN reproduce the excitatory influence of PVN on vagus-responsive NTS neurons, and the responses featured a prolonged activation of NTS neurons following cessation of PVN stimuli. We speculate that such results support the possibility that recurrent PVN projections to NTS might contribute to the observed drastically reduced sAP activity by the KC intervention. Both of these PVN-associated peptides strongly alter presynaptic release of vagal afferent glutamate on NTS second order neurons (Bailey et al., 2006; Peters et al., 2008).

Transformation of vagal afferent signaling.

Overall, our studies were based in direct electrical activation of vagal afferent axons and have identified major changes in vagal signaling that occur at second and higher order NTS neurons during and following VNS treatment. Our protocols cannot identify the destination of NTS projections nor the identity of supramedullary-linking neurons, but KC results clearly implicated contributions of supramedullary neurons. In the intact functioning system, physiological conditions will activate vagal afferents, and these stimuli will be quite different in pattern and timing than our electrical stimulation. Clearly, we cannot distinguish from these studies whether changes in afferent transmission reflected a removal of an excitatory influence or an augmentation of inhibition nor distinguish a presynaptic afferent action from a postsynaptic mechanism. The spread of excitation from A-fiber vagal afferent pathways to C-fiber and polysynaptic pathways depended on pathways descending from supramedullary neurons. Together, our KC findings uncover substantial augmentation of both the second order transmission of vagal afferent information as well as the reverberant spread of excitation to additional indirect pathways within NTS. This finding is critical for helping establish optimal VNS parameters to treat chronic diseases like heart failure and epilepsy since the activation of these supramedullary nuclei with VNS will, in turn, influence different regions of the brain including NTS.

Implications of the A-fiber dependence of VNS.

A prominent finding of our VNS therapy-mimicking design relied on weak stimuli that directly activate A-fiber vagal afferents only. A-fiber afferents are a very minor anatomical component of the cervical vagus, and yet this small group of afferents dominates normal

organ control because they are active under physiological conditions (Andresen et al., 2012). By driving A-fiber afferents with VNS, we found that the normal pathway segregation of direct A-fiber information from direct C-fiber pathways was violated. These relations are discriminated by the timing of events. However, the appearance of sAPs on Mono C-fiber second order and Poly NTS neurons resulted from indirect activation that entirely depended on A-fiber activation of neurons outside of the brainstem. This observation raises important questions about the initiating source of increased activity in NTS neurons weakly time-linked to VNS in the intact system. This out-of-sync yet VNS-dependent activation of NTS more widely represents an amplification of the VNS A-fiber viscerosensory signal. With prolonged periods of A-fiber Mono NTS neuron activation, a subset of C-fiber Mono and Poly NTS neurons fire APs no longer synchronous with the original direct activation. It is not clear what contributions this dispersion of VNS excitation makes to therapeutic efficacy or in which organ-level control pathways such neurons might participate; however, the implication is that prolonged VNS of the therapeutic-style regimen can then recruit much more broadly. Although we cannot independently identify the sensory modality of the A-fiber vagal afferents recruited, the electrical stimuli activated all A-fibers so that multiple modalities and organ origins of vagal afferents are likely activated, as well as the pathways that they normally regulate. This may well be the reason that VNS impacts such a broad array of brain systems. Perhaps the most valuable implication, however, may be that this work indicates a potential path to more rationally formulate therapeutic VNS protocols informed by A-fiber discharge and pathway characteristics. Would much lower intensities recruit fewer A-fibers but be equally effective? Half BI stimuli recruited sAPs in C-fiber Mono neurons in our previous studies (Beaumont et al., 2017), suggesting that submaximal activation recruits sufficient vagal A-fiber NTS neurons to induce supramedullary neuronal activity. Would the faster conduction speed of A-fibers allow for better VNS designs of brief bursts repeated less often that would be equally or more effective? Do some pathways and outcomes prefer different paradigms? These are just a few of the questions that deserve careful evaluation and additional model systems for testing beyond this first stage of vagal afferent processing.

Acknowledgements

The authors would like to acknowledge Dr. Nicole Lewis, PhD for revising the final statistical analyses of the data presented in this paper.

Funding

National Heart, Lung and Blood Institute (NHLBI) R01HL141560 (Beaumont)

These funding sources had no role in the study design, collection, analysis and interpretation of data; in the writing of the article; nor in the decision to submit the article for publication.

Data availability statement

All data generated or analyzed for this study are included in the figures or statistical summary document for this published article.

References

Affleck VS, Coote JH & Pyner S (2012). The projection and synaptic organisation of NTS afferent connections with presympathetic neurons, GABA and nNOS neurons in the paraventricular nucleus of the hypothalamus. Neuroscience 219(1-2): 48–61. [PubMed: 22698695]

Andresen MC, Hofmann ME & Fawley JA (2012). The unsilent majority-TRPV1 drives "spontaneous" transmission of unmyelinated primary afferents within cardiorespiratory NTS. Am. J. Physiol Regul. Integr. Comp Physiol 303(12): R1207–R1216. [PubMed: 23076872]

Andresen MC & Kunze DL (1994). Nucleus tractus solitarius--gateway to neural circulatory control. Annu. Rev. Physiol 56: 93–116. [PubMed: 7912060]

Andresen MC & Paton JF (2011). The nucleus of the solitary tract: Processing information from viscerosensory afferents. Central Regulation of Autonomic Functions, 2nd edition. Llewellyn-Smith J and Verberne AJ, Oxford

Bailey TW, Hermes SM, Andresen MC & Aicher SA (2006). Cranial visceral afferent pathways through the nucleus of the solitary tract to caudal ventrolateral medulla or paraventricular hypothalamus: target-specific synaptic reliability and convergence patterns. J. Neurosci 26(46): 11893–11902. [PubMed: 17108163]

Bailey TW, Hermes SM, Whittier KL, Aicher SA & Andresen MC (2007). A-type potassium channels differentially tune afferent pathways from rat solitary tract nucleus to caudal ventrolateral medulla or paraventricular hypothalamus. J. Physiol 582(Pt 2): 613–628. [PubMed: 17510187]

Bailey TW, Jin YH, Doyle MW, Smith SM & Andresen MC (2006). Vasopressin inhibits glutamate release via two distinct modes in the brainstem. J. Neurosci 26(23): 6131–6142. [PubMed: 16763021]

Beaumont E, Campbell RP, Andresen MC, Scofield S, Singh K, Libbus I, KenKnight BH, Snyder L & Cantrell N (2017). Cervical vagus nerve stimulation augments spontaneous discharge in second- and higher-order sensory neurons in the rat nucleus of the solitary tract. Am J Physiol Heart Circ Physiol 313(2): H354–H367. [PubMed: 28476920]

Beaumont E, Salavatian S, Southerland EM, Vinet A, Jacquemet V, Armour JA & Ardell JL (2013). Network interactions within the canine intrinsic cardiac nervous system: implications for reflex control of regional cardiac function. J. Physiol 591(Pt 18): 4515–4533. [PubMed: 23818689]

Beaumont E, Southerland EM, Hardwick JC, Wright GL, Ryan S, Li Y, KenKnight BH, Armour JA & Ardell JL (2015). Vagus nerve stimulation mitigates intrinsic cardiac neuronal and adverse myocyte remodeling postmyocardial infarction. Am. J Physiol Heart Circ. Physiol 309(7): H1198–H1206. [PubMed: 26276818]

Beaumont E, Wright GL, Southerland EM, Li Y, Chui R, KenKnight BH, Armour JA & Ardell JL (2016). Vagus nerve stimulation mitigates intrinsic cardiac neuronal remodeling and cardiac hypertrophy induced by chronic pressure overload in guinea pig. Am. J Physiol Heart Circ. Physiol 310(10): H1349–H1359. [PubMed: 26993230]

Bonaz B, Picq C, Sinniger V, Mayol JF & Clarençon D (2013). Vagus nerve stimulation: from epilepsy to the cholinergic anti-inflammatory pathway. Neurogastroenterol Motil 25(3): 208–221. [PubMed: 23360102]

Byku M & Mann DL (2016). Neuromodulation of the failing heart: lost in translation? JACC. Basic Transl. Sci 1(3): 95–106. [PubMed: 27525317]

Cersosimo MG & Benarroch EE (2013). Central control of autonomic function and involvement in neurodegenerative disorders. Handb Clin Neurol 117: 45–57. [PubMed: 24095115]

Cunningham JT, Mifflin SW, Gould GG & Frazer A (2008). Induction of c-Fos and DeltaFosB immunoreactivity in rat brain by Vagal nerve stimulation. Neuropsychopharmacology 33(8): 1884–1895. [PubMed: 17957222]

DiCarlo L, Libbus I, Amurthur B, KenKnight BH & Anand IS (2013). Autonomic regulation therapy for the improvement of left ventricular function and heart failure symptoms: the ANTHEM-HF study. J Card Fail 19(9): 655–660. [PubMed: 24054343]

DiCarlo LA, Libbus I, Kumar HU, Mittal S, Premchand RK, Amurthur B, KenKnight BH, Ardell JL & Anand IS (2018). Autonomic regulation therapy to enhance myocardial function in heart failure patients: the ANTHEM-HFpEF study. ESC Heart Fail 5(1): 95–100. [PubMed: 29283224]

Doyle MW & Andresen MC (2001). Reliability of monosynaptic sensory transmission in brain stem neurons in vitro. J. Neurophysiol 85(5): 2213–2223. [PubMed: 11353036]

Englot DJ, Rolston JD, Wright CW, Hassnain KH & Chang EF (2016). Rates and Predictors of Seizure Freedom With Vagus Nerve Stimulation for Intractable Epilepsy. Neurosurgery 79(3): 345–353. [PubMed: 26645965]

Fawley JA, Hegarty DM, Aicher SA, Beaumont E & Andresen MC (2021). Dedicated C-fiber vagal sensory afferent pathways to the paraventricular nucleus of the hypothalamus. Brain Res 1769: 147625. [PubMed: 34416255]

Gasparini S, Howland JM, Thatcher AJ & Geerling JC (2020). Central afferents to the nucleus of the solitary tract in rats and mice. J Comp Neurol 528(16): 2708–2728. [PubMed: 32307700]

Geerling JC, Shin JW, Chimenti PC & Loewy AD (2010). Paraventricular hypothalamic nucleus: axonal projections to the brainstem. J Comp Neurol 518(9): 1460–1499. [PubMed: 20187136]

Gonzalez IE, Ramirez-Matias J, Lu C, Pan W, Zhu A, Myers MG & Olson DP (2021). Paraventricular Calcitonin Receptor Expressing Neurons Modulate Energy Homeostasis in Male Mice. Endocrinology.

Johnson RL & Wilson CG (2018). A review of vagus nerve stimulation as a therapeutic intervention. J Inflamm Res 11: 203–213. [PubMed: 29844694]

Kannan H & Yamashita H (1985). Connections of neurons in the region of the nucleus tractus solitarius with the hypothalamic paraventricular nucleus: their possible involvement in neural control of the cardiovascular system in rats. Brain Res 329(1-2): 205–212. [PubMed: 3978442]

Karimnamazi H, Travers SP & Travers JB (2002). Oral and gastric input to the parabrachial nucleus of the rat. Brain Res 957(2): 193–206. [PubMed: 12445962]

Kawabe T, Chitravanshi VC, Kawabe K & Sapru HN (2008). Cardiovascular function of a glutamatergic projection from the hypothalamic paraventricular nucleus to the nucleus tractus solitarius in the rat. Neuroscience 153(3): 605–617. [PubMed: 18424005]

Kawai Y (2018). Differential Ascending Projections From the Male Rat Caudal Nucleus of the Tractus Solitarius: An Interface Between Local Microcircuits and Global Macrocircuits. Front Neuroanat 12: 63. [PubMed: 30087599]

Landgraf R, Malkinson T, Horn T, Veale WL, Lederis K & Pittman QJ (1990). Release of vasopressin and oxytocin by paraventricular stimulation in rats. Am J Physiol 258(1 Pt 2): R155–159. [PubMed: 2301628]

Lee JS, Morrow D, Andresen MC & Chang KS (2002). Isoflurane depresses baroreflex control of heart rate in decerebrate rats. Anesthesiology 96(5): 1214–1222. [PubMed: 11981163]

Libbus I, Nearing BD, Amurthur B, KenKnight BH & Verrier RL (2016). Autonomic regulation therapy suppresses quantitative T-wave alternans and improves baroreflex sensitivity in patients with heart failure enrolled in the ANTHEM-HF study. Heart Rhythm 13(3): 721–728. [PubMed: 26601770]

Loewy AD (1990). Central autonomic pathways. In Central regulation of autonomic functions. Loewy AD and Spyer KM, Oxford University Press, New York: 88–103.

McDougall SJ & Andresen MC (2013). Independent transmission of convergent visceral primary afferents in the solitary tract nucleus. J. Neurophysiol 109(2): 507–517. [PubMed: 23114206]

Miles R (1986). Frequency dependence of synaptic transmission in nucleus of the solitary tract in vitro. J Neurophysiol 55(5): 1076–1090. [PubMed: 3012009]

Nearing BD, Libbus I, Amurthur B, KenKnight BH & Verrier RL (2016). Acute autonomic engagement assessed by heart rate dynamics during vagus nerve stimulation in patients with heart failure in the ANTHEM-HF trial. J Cardiovasc. Electrophysiol.

Paxinos G & Watson C, Eds. (1986). The rat brain in stereotaxic coordinates. 2nd ed. New York; Academic Press.

Paxinos G, Watson C, Pennisi M & Topple A (1985). Bregma, lambda and the interaural midpoint in stereotaxic surgery with rats of different sex, strain and weight. J Neurosci Methods 13(2): 139–143. [PubMed: 3889509]

Peters JH, McDougall SJ, Kellett DO, Jordan D, Llewellyn-Smith IJ & Andresen MC (2008). Oxytocin enhances cranial visceral afferent synaptic transmission to the solitary tract nucleus. J. Neurosci 28(45): 11731–11740. [PubMed: 18987209]

Premchand RK, Sharma K, Mittal S, Monteiro R, Dixit S, Libbus I, DiCarlo LA, Ardell JL, Rector TS, Amurthur B, KenKnight BH & Anand IS (2014). Autonomic regulation therapy via left or right cervical vagus nerve stimulation in patients with chronic heart failure: results of the ANTHEM-HF trial. J. Card Fail 20(11): 808–816. [PubMed: 25187002]

Premchand RK, Sharma K, Mittal S, Monteiro R, Dixit S, Libbus I, DiCarlo LA, Ardell JL, Rector TS, Amurthur B, KenKnight BH & Anand IS (2016). Extended follow-up of patients with heart failure receiving autonomic regulation therapy in the ANTHEM-HF study. J Card Fail 22(8): 639–642. [PubMed: 26576716]

Ruyle BC, Klutho PJ, Baines CP, Heesch CM & Hasser EM (2018). Hypoxia activates a neuropeptidergic pathway from the paraventricular nucleus of the hypothalamus to the nucleus tractus solitarii. Am J Physiol Regul Integr Comp Physiol 315(6): R1167–R1182. [PubMed: 30230933]

Sawchenko PE & Swanson LW (1983). The organization and biochemical specificity of afferent projections to the paraventricular and supraoptic nuclei. Prog. Brain Res 60: 19–29. [PubMed: 6198687]

Scheuer DA, Zhang J, Toney GM & Mifflin SW (1996). Temporal processing of aortic nerve evoked activity in the nucleus of the solitary tract. J. Neurophysiol 76(6): 3750–3757. [PubMed: 8985873]

Schwartz PJ, La Rovere MT, De Ferrari GM & Mann DL (2015). Autonomic modulation for the management of patients with chronic heart failure. Circ. Heart Fail 8(3): 619–628. [PubMed: 25991804]

Seki A, Green HR, Lee TD, Hong L, Tan J, Vinters HV, Chen PS & Fishbein MC (2014). Sympathetic nerve fibers in human cervical and thoracic vagus nerves. Heart Rhythm.

Sofroniew MV, Weindl A, Schrell U & Wetzstein R (1981). Immunohistochemistry of vasopressin, oxytocin and neurophysin in the hypothalamus and extrahypothalamic regions of the human and primate brain. Acta Histochem Suppl 24: 79–95. [PubMed: 6785843]

Ulrich-Lai YM & Herman JP (2009). Neural regulation of endocrine and autonomic stress responses. Nat Rev Neurosci 10(6): 397–409. [PubMed: 19469025]

van der Kooy D, Koda LY, McGinty JF, Gerfen CR & Bloom FE (1984). The organization of projections from the cortex, amygdala, and hypothalamus to the nucleus of the solitary tract in rat. J Comp Neurol 224(1): 1–24. [PubMed: 6715573]

Yamashita H, Kannan H, Kasai M & Osaka T (1987). Decrease in blood pressure by stimulation of the rat hypothalamic paraventricular nucleus with L-glutamate or weak current. J Auton Nerv Syst 19(3): 229–234. [PubMed: 2887610]

Zhukova GP (1980). The afferent pathway to the locus coeruleus from the nucleus of the solitary tract. Neurosci Behav Physiol 10(1): 27–32. [PubMed: 7383321]

Key Points

- Vagus nerve stimulation is routinely used in the clinic to treat epilepsy and depression, despite our uncertainty about how this treatment works.
- For this study, the connections between NTS and the higher brain regions were severed to learn more about their contribution to activity of these neurons during stimulation.
- Severing these brain connections reduced baseline activity as well as reducing stimulation-induced activation for NTS neurons receiving myelinated vagal input.
- Higher brain regions play a significant role in maintaining both normal activity in NTS as well as indirect mechanisms of enhancing NTS neuronal activity during vagus nerve stimulation.

New and Noteworthy:

Clinically-styled vagus nerve stimulation (VNS) activated only myelinated vagal afferents to elevate activity in neurons located in the caudomedial nucleus of the solitary tract (NTS). Surprisingly, only a portion of the increased activity in NTS neurons was due to direct activation, but substantial increases also resulted from indirect activation at both C-fiber-innervated 2nd order as well as higher order NTS neurons. A mid-collicular knife cut strongly attenuated the activity generated by VNS, thereby suggesting that supramedullary neurons have a significant role in maintaining both the normal vagal afferent responsiveness as well as the indirect pathways by which vagal activation enhanced NTS activity.

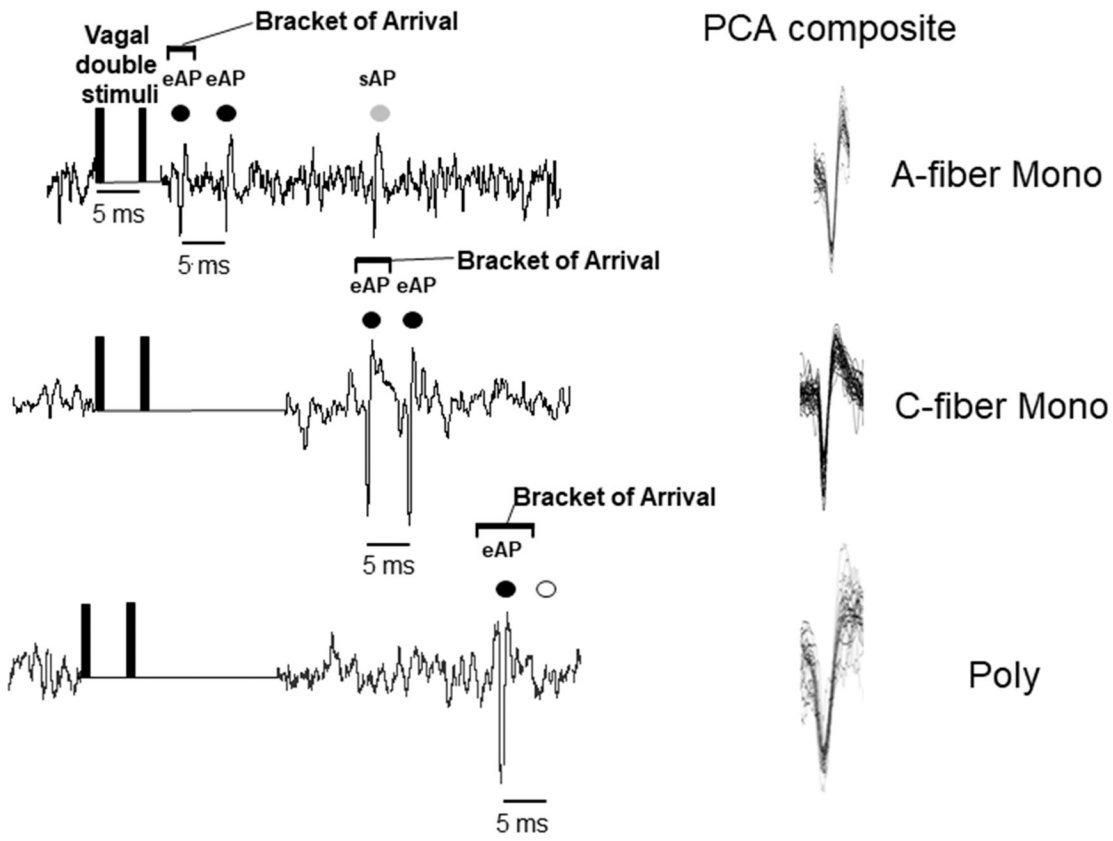

Fig. 1.

Identification of unique action potentials (APs) belonging to a single NTS neuron relied on principal component analysis (PCA) and separation of monosynaptic A- or C-fiber from polysynaptic conduction pathways. High-intensity double electrical stimuli to the cervical vagus (supramaximal, see Methods) triggered APs within NTS neurons. The timing behavior of these APs fell into three classes. Paired vagal electrical stimuli activated early arriving APs that were consistent with myelinated monosynaptic vagal A-fibers (A-fiber Mono, top). Repeated trials were collected in order to populate each PCA composite identifying the AP signature of each recorded unique NTS neuron (right). The Bracket of Arrival defines the latency range for an individual neuron triggered by vagal electrical stimuli (eAP). Latency is defined as the conduction time required to travel from the cervical stimulation point to generating an NTS eAP. The double electrical stimuli (interval of 5 ms) unfailingly evoked two successful APs (eAP, filled black circles ●) appearing at relatively fixed times and thus confirmed that the vagal pathway was monosynaptic. Note that APs falling outside of the Bracket of Arrival but satisfying the PCA template were considered spontaneous (sAP, filled grey circles ●) and not triggered by the vagal stimulus. Later-arriving eAPs due to slower conduction along an unmyelinated afferent pathway but monosynaptically consistent in their timing and paired electrical stimuli responses (filled black circles, ●) were classed as monosynaptic C-fiber events (C-fiber Mono, middle). Failures to evoke time-synced APs (unfilled circle, ○) in response to the paired vagal electrical stimuli indicated that vagal activation followed a polysynaptic pathway to the recorded NTS neuron (Poly, bottom). Note PCAs all have APs time-aligned at the peak downward deflection here and throughout.

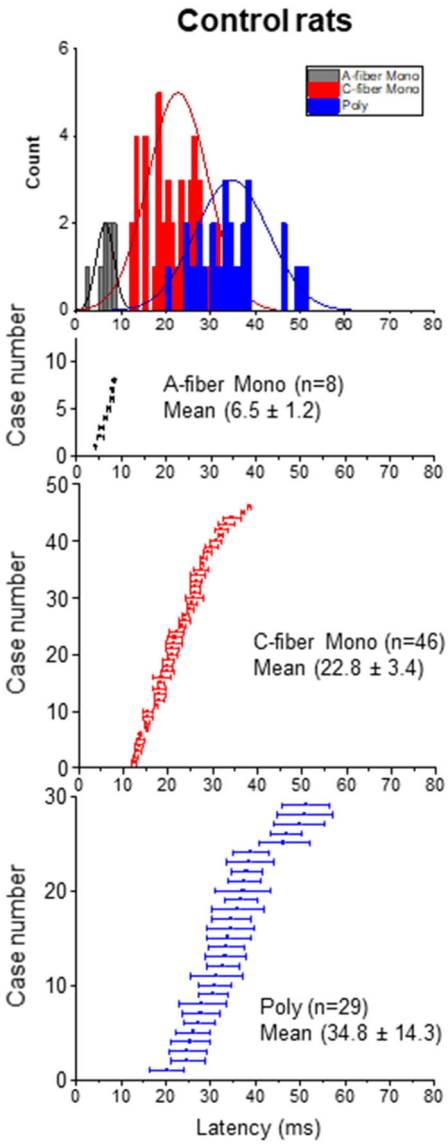

Fig. 2.

Summary distributions of all recorded NTS neurons in Control rats with eAPs by class: A-fiber Mono (gray), C-fiber Mono (red) and Poly (blue) in the top panel with fit lines showing normal distributions of sampled latencies – total of 83 neurons from 10 rats. The lower three panels show the individual AP response latencies across each pathway class measured for the 20 supramaximal vagal electrical stimuli. The A-fiber Mono event paths (n=8 from 7/8 rats) had the shortest mean latencies and ranged very narrowly between 2.3 and 8.4 ms. The SD error bars are represented as horizontal brackets representing the jitter in the monosynaptic latency within each neuron and were demonstrably consistent for A-fiber Mono pathways, averaging 1.2 ms (jitter, SD of latency over 20 iterations). The jitter SDs are so narrow for the A-fiber Monos that they are more difficult to discern. In contrast, C-fiber Mono pathways (n=46 from 10 rats) arrived later and spread across a wider range (12.5 to 38.2 ms) with larger jitters averaging 3.4 ms. The distributions of the APs failing the paired electrical stimuli test were identified pathways as Poly (n=29 from 10 rats) and

had very large jitters ranging from 20.2 to 51.3 ms. Latency distributions of the C-fiber Monos and Polys overlapped, making the vagal paired electrical stimuli test essential for discriminating pathways.

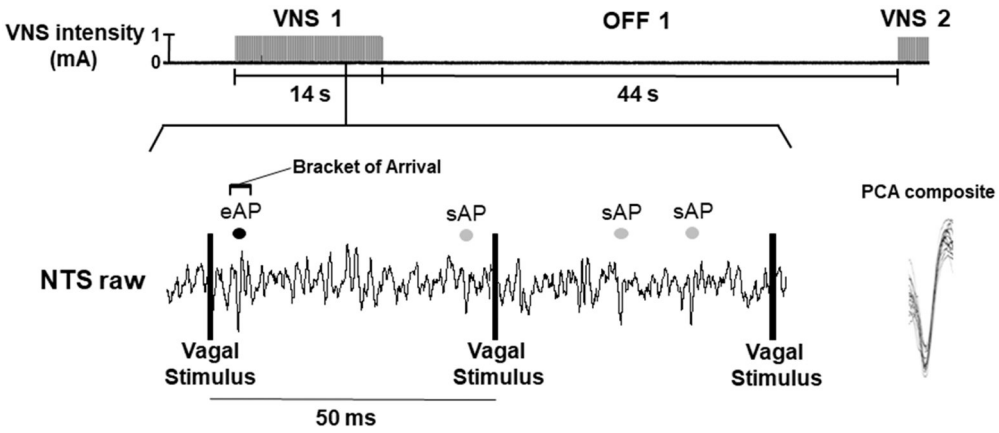

Fig. 3.

VNS treatment stimuli characteristically triggered eAP and sAP responses in a representative A-fiber Mono NTS neuron. The VNS protocol consisted of bursts of vagus electrical stimuli (e.g. VNS 1, 14 s), followed by periods of no stimulation (e.g. OFF 1, 44 s). Five VNS cycles were delivered. VNS was delivered at a low intensity (BI, see Methods), determined in each animal by the bradycardia test, and at 20 Hz (50 ms vagal electrical stimulus interval). Thus, VNS intensity was much lower here than the supramaximal intensity previously used for pathway discrimination (Figs. 1-2). Only the first cycle (VNS 1 and OFF 1) is fully displayed here (for clarity). The lower panel displays an expanded time sweep (taken from the time indicated by the vertical line) depicting responses of a representative NTS neuron monosynaptically connected to an A-fiber pathway (see Methods). At BI, VNS directly elicited an eAP that fell within the characteristic Bracket of Arrival for this neuron (between 6.7 and 8.6 ms), but the middle stimulus failed to evoke an AP in the characteristic time frame in this example. APs falling within this time bracket were considered eAPs directly linked to the vagal stimulus pulse within VNS (filled black circles, ●). The success rate of A-fiber Mono neurons varied across the vagal burst of stimuli and failures were evident mixed together with unsynchronized sAPs that fell outside of that Bracket of Arrival (filled grey circles, ●). All analyzed APs conformed to the PCA composite for the displayed neuron (right).

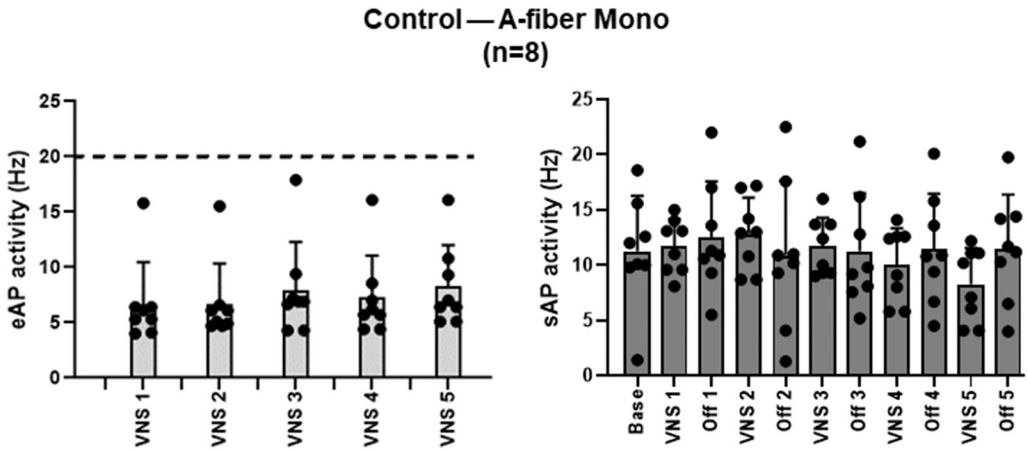

Fig. 4.

The overall AP mean responses to VNS held constant on average across each of five VNS cycles for A-fiber Mono NTS neurons in Control rats. Counting all eAPs within VNS 1 through VNS 5 showed no consistent differences across the protocol (ANOVA, NS, P = 0.1525). Likewise, the sAP counts across the five VNS periods were steady for both active stimulation (VNS 1-5), as well as the off periods (Off 1-5). None of the sAP counts were different from the baseline activity (Base) (ANOVA, NS, P = 0.2978) – total of 8 neurons from 7 rats. Neuronal activity was expressed as the APs detected divided by the respective period duration and given as activity rate in spikes/s or Hz. The horizontal dotted line at 20 Hz indicates the VNS frequency delivered.

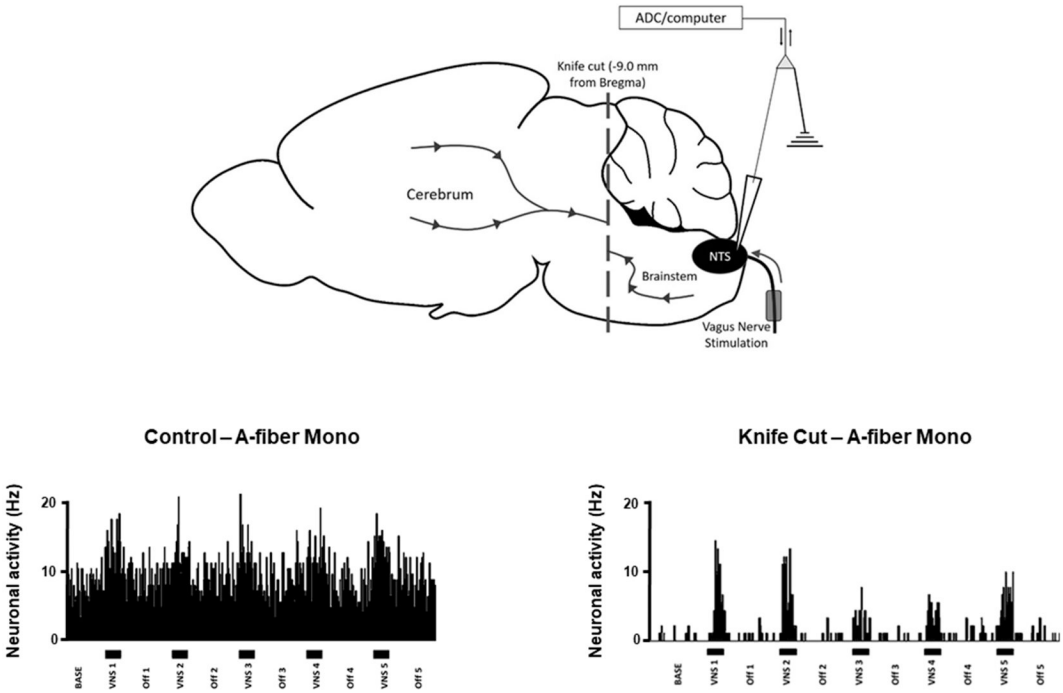

Fig. 5.

Brain knife cuts (KC) separated the brainstem from the forebrain and resulted in greatly reduced NTS activity as well as VNS responses. The mid-collicular KC was centered at 9 mm caudal to Bregma – well rostral of the caudal NTS recording area. This KC eliminated all ascending and descending neuronal connections between the brainstem and the cerebrum (top image). Two different representative NTS neurons received A-fiber Mono conducting vagal pathways, one from a Control animal (left) and a second from an animal following the KC. Both examples show robust direct eAP activation during VNS periods despite much lower overall activities in the KC rat. Each black bar above VNS 1-5 on the x-axis represents 14 s (VNS 1-5), and each white space represents 44 s (BASE, Off 1-5).

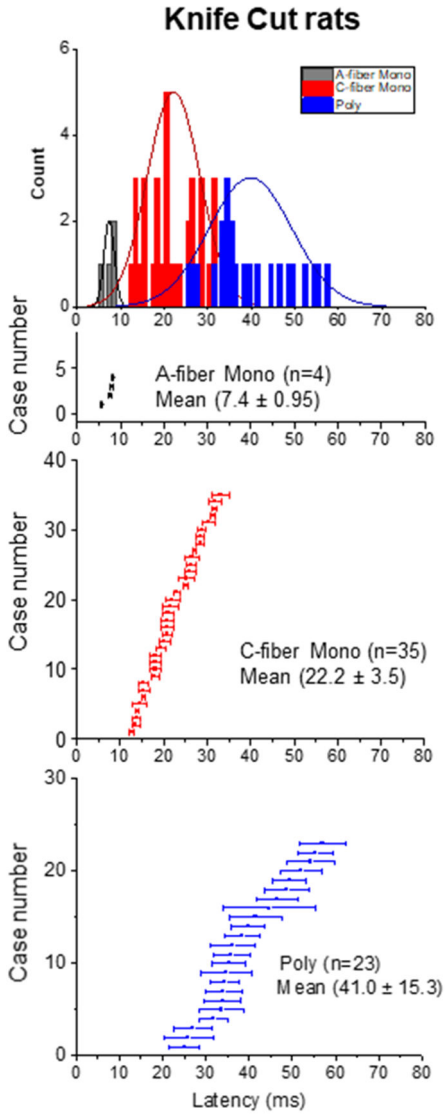

Fig. 6.

Summary distributions of all recorded NTS neurons with vagal eAPs by class for KC rats: A-fiber Mono (gray), C-fiber Mono (red) and Poly (blue) in the top panel, with fit lines showing normal distributions of sampled latencies – total of 62 KC NTS neurons from 10 rats. The A-fiber Mono event paths (n=4 from 4 rats) had the shortest mean latencies: very narrowly ranging between 5.7 and 8.3 ms and an average jitter of 1.0 ms. Horizontally-plotted jitter SDs are so narrow for the A-fiber Monos that they are more difficult to discern. C-fiber Mono pathways (n=35 from 10 rats) arrived later and spread across a wide range (12.7 to 33.1 ms) with an average jitter of 3.5 ms. The distributions of the APs failing the paired electrical stimuli test were identified as Poly pathways (n=23 from 10 rats) having a wider range of (29.3 to 69.1 ms) and a very large jitter of 15.3 ms. Latencies and jitters for each NTS class were not different compared to the Control group (Figure 2) for A-fiber Mono (*t* test, NS, P = 0.4015), C-fiber Mono (*t* test, NS, P = 0.7051) and Poly (*t* test, NS,

P = 0.1525). Therefore, latencies, jitters and paired electrical stimuli for NTS classification were used to compare Control vs KC rats.

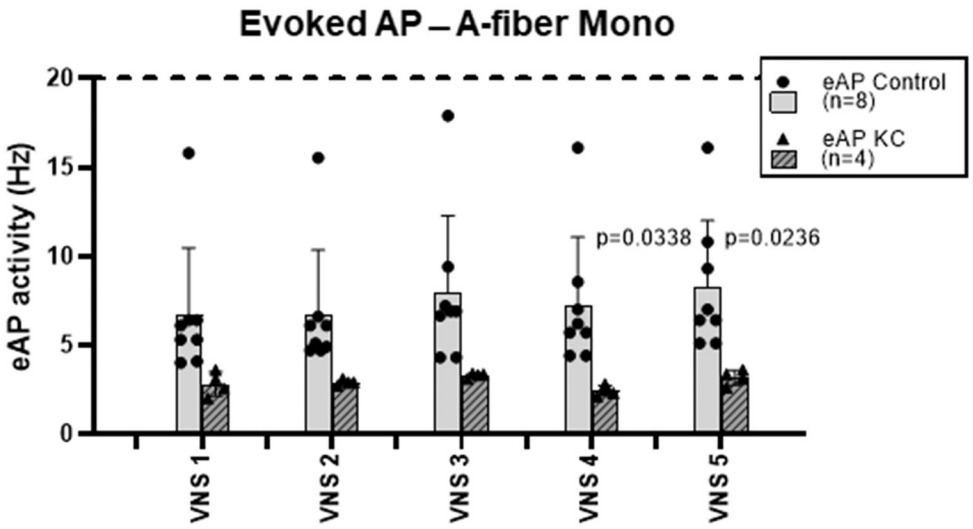

Fig. 7.

KC rats had fewer eAPs (n=4 neurons from 4 rats) than Control rats (n=8 neurons from 7 rats) for NTS neurons receiving A-fiber Mono pathways. Thus, KC greatly lowers vagal afferent successful excitation of A-fiber Mono NTS neurons. The horizontal dotted line at 20 Hz indicates the VNS treatment frequency. ANOVA, $P < 0.0001$ followed by Dunnett's Test.

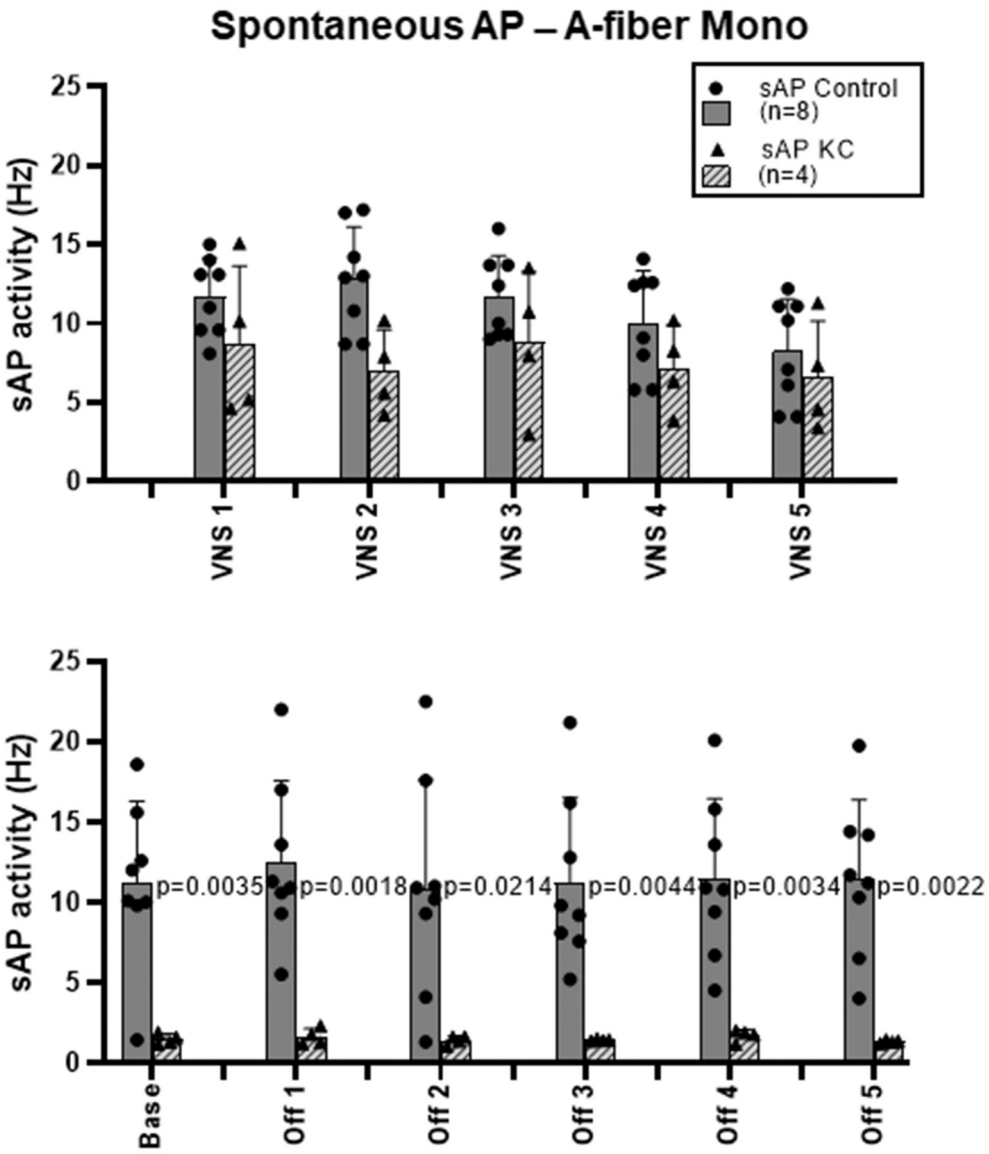

Fig. 8.

KC (n=4 neurons from 4 rats) reduced spontaneous activity (sAP) in A-fiber Mono NTS neurons compared to Controls (n=8 neurons from 8 rats) in both Base and Off periods 1-5 with ANOVA $P < 0.0001$ followed by Dunnett's Test (bottom graph). In contrast, active periods of VNS stimulation had similar levels regardless of KC (upper graph).

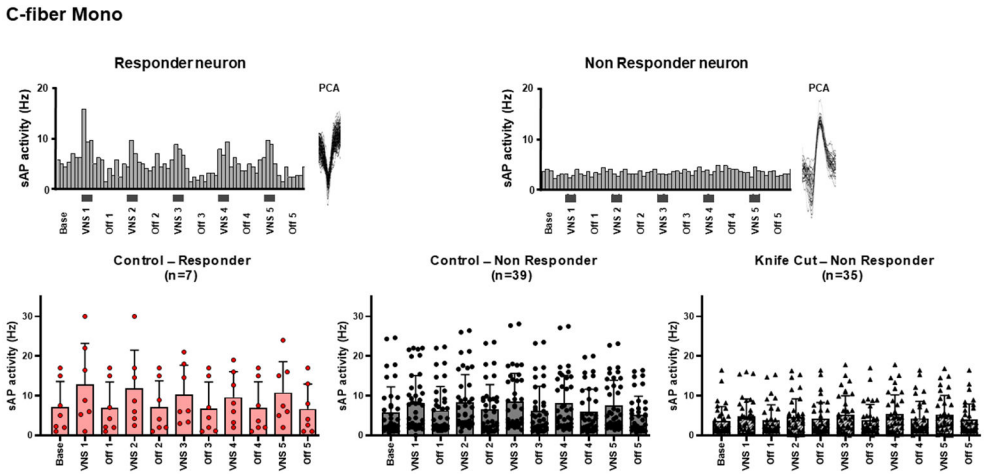

Fig. 9.

C-fiber Mono NTS neurons were monosynaptically activated by high-intensity test electrical stimuli (insets PCA right panels), but were not activated by the weak, subthreshold BI used for VNS. Nonetheless, VNS augmented sAP activity in some C-fiber Mono NTS neurons. In Controls, 7 out of 46 neurons (~15%) from 10 rats were classified as Responder neurons, meaning that sAP increased by > 30% during VNS compared to base (representative example on upper left panel, activity across time for Control Responders shown in lower left panel). The bursts of sAPs aligned with the intervals of active VNS, but APs were identified as spontaneous and not directly evoked using the characteristic Bracket of Arrival for each neuron. VNS failed to affect discharge in most C-fiber Mono-innervated NTS neurons (Non Responder, representative example on upper right panel, activity across time for Control Non Responders shown in lower middle panel). In KC rats, all C-fiber Mono-innervated NTS neurons were Non Responders (n=35 from 10 rats, lower right panel). Each black bar above VNS 1-5 on the x-axis represents 14 s (VNS 1-5), and each white space represents 44 s (Base, Off 1-5). For control responders: Base vs VNS 1-5, ANOVA, NS, P = 0.4077; Base vs Off 1-5, ANOVA, NS, P = 1.

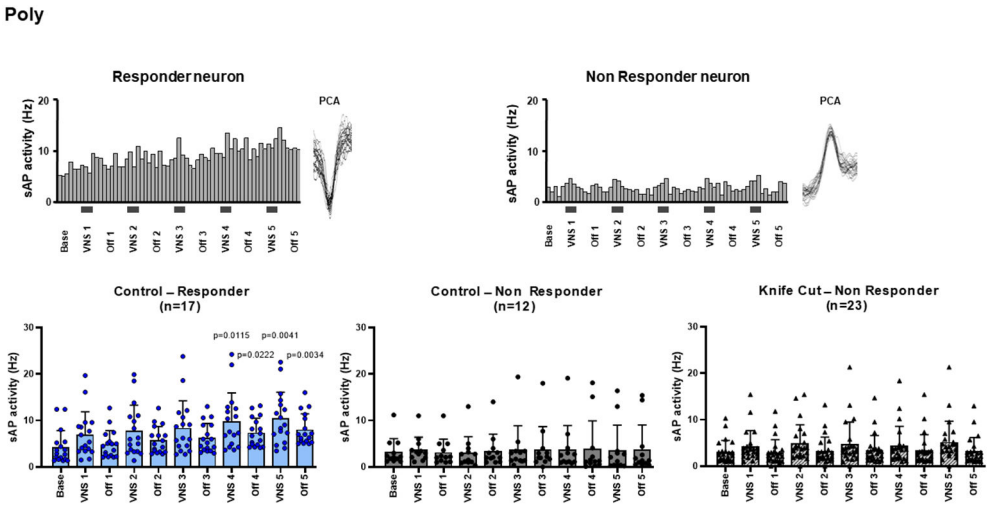

Fig. 10.

NTS neurons that are connected to the vagal afferents indirectly are considered Poly in network organization. VNS increased activity in most (~60%) higher order NTS neurons (n=17) in 10 Control rats and were deemed Responders (lower left panel), while the remaining Poly neurons were deemed Non Responders (n=12 neurons from 10 Control rats, lower middle panel). For KC rats, all Poly neurons (n=23 neurons from 10 rats) were Non Responders (lower right panel). The upper panels show a representative example from one Responder neuron (left) and one Non Responder neuron (right) during 5 cycles of VNS. The individual PCAs are illustrated on the right side of each example. These Poly NTS neurons only showed sAPs since none of them were temporally-linked to vagal electrical stimuli. Each black bar above VNS 1-5 on the x-axis represents 14 s (VNS 1-5), and each white space represents 44 s (Base, Off 1-5). For control responders: Base vs VNS 1-5, ANOVA P = 0.0138; Base vs Off 1-5, ANOVA P = 0.0053, followed by Dunnett's Test.

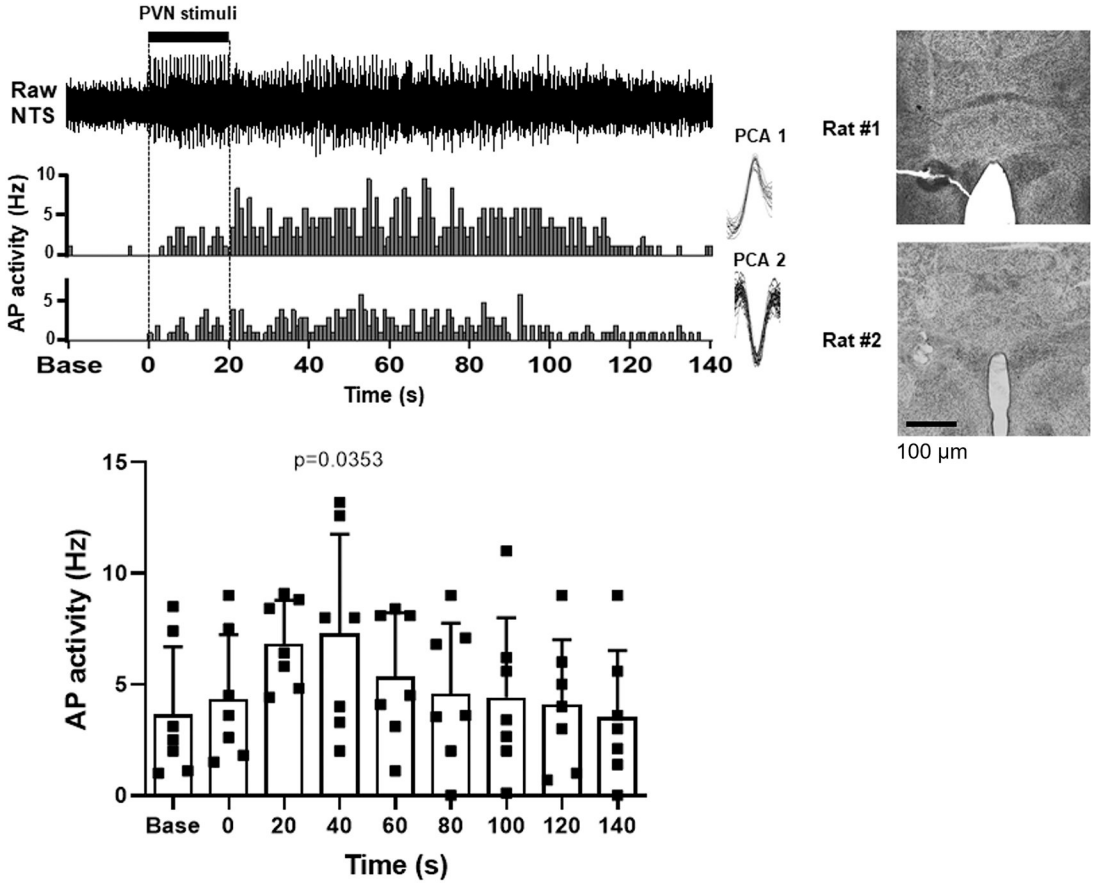

Fig. 11.

Direct activation of neurons in the paraventricular nucleus of the hypothalamus (PVN) activated most (7/12) NTS neurons from 3 rats. In two representative examples (upper panels), electrical activation of PVN at 1 Hz for 20 s with an intensity of 100 µA increased AP activity in both NTS neurons. 5 out of 12 NTS neurons did not show any changes in activity during PVN stimulation. The lower panel plots the aggregate activity of the 7 neurons that responded to stimulation. Base activity was measured for 20 s before PVN activation. PVN electrical stimuli were then delivered during 20 s (time 0-20 s), and the average NTS activity was elevated beginning immediately after PVN stimulation (time 20 s). That elevated aggregate activity was maintained for an additional 20 s after PVN electrical stimulation ceased (time 40 s). * *t* test, base vs 40 s, P = 0.0353. An electrolytic lesion using 25 µA anodal current with 120 s duration were performed following PVN stimulation to confirm electrode placement. The lesion is visible in the lateral portion of the left PVN from 2 rats (4x photomicrographs shown on right).